Journal of Alloys and Compounds 520 (2012) 287–294

Contents lists available at SciVerse ScienceDirect

Journal of Alloys and Compounds

journal homepage: www.elsevier.com/locate/jallcom

Effect of cold rolling on hydrogen sorption properties of die-cast and as-cast magnesium alloys

S. Amira [a], J. Huot [b,*]

[a] Aluminium Technology Centre, Industrial Materials Institute, National Research Council Canada, 501, Boul. de l'Université Est, Saguenay, Québec, Canada G7H 8C3
[b] Institut de Recherche sur l'Hydrogène, Université du Québec à Trois-Rivières, 3351, Boul. des Forges, Trois-Rivières, Québec, Canada G9A 5H7

ARTICLE INFO

Article history:
Received 14 November 2011
Received in revised form 6 January 2012
Accepted 9 January 2012
Available online 15 January 2012

Keywords:
Severe Plastic Deformation (SPD)
Magnesium alloys
Hydrogen storage
Casting

ABSTRACT

The effect of cold rolling, as an activation process of materials aimed to hydrogen storage application, was applied to some cast magnesium alloys. The alloys studied in this work are AZ91D and three experimental creep resistant magnesium alloys (MRI153, AXJ530, ZAEX10430) in the as-cast and die-cast states. Experiments showed that AZ91D, MRI153 and ZAEX10430 have faster absorption/desorption kinetic than as-cast pure magnesium. On the other hand, AXJ530 showed the worst hydrogen storage properties. These results were attributed to a possible beneficial effect of aluminum and zinc as alloying elements. Segregation inside primary α-Mg grains may explain the difference of hydrogen storage properties between as-cast and die-cast alloys.

1. Introduction

For hydrogen storage applications, magnesium is considered as a good candidate because of its large hydrogen storage capacity (7.6 wt.%), low cost and high abundance in the earth's crust. Besides, the magnesium based hydrides possess other interesting properties, such as reversibility and recyclability. Unfortunately, the reaction of magnesium with hydrogen is characterized by a high thermodynamic stability which leads to a poor absorption–desorption kinetics, and high temperatures of operation (300 °C). This is far from the target set by the US Department of Energy (DOE) for a dehydrogenation temperature between 60 and 120 °C for commercial viability [1]. In this context, many efforts have been made recently in order to improve the hydrogenation properties of magnesium, such as appropriate alloying of magnesium [2–4], adding catalyst [5], and manufacturing nanocrystalline powder [6].

It has been shown recently that repeated cold rolling (CR) could be applied to process hydrogen storage alloys, mainly magnesium and magnesium-based alloys [7–11]. Cold rolling (CR) was proposed as an alternative to mechanical ball milling in order to facilitate hydrogenation by creating many lattice defects (such as point defects and dislocations) on the surface and in the bulk. It is thought that these lattice defects promote the diffusion of hydrogen by providing many sites with low activation energy of diffusion. The induced microstrain might assist diffusion by reducing the hysteresis of hydrogen absorption and desorption [12].

In this paper, we report the investigation of the effect of repeated cold rolling on the structure and hydrogen storage properties of four magnesium alloys as measured in the as-cast and the die-cast states. These alloys are: (1) commercial AZ91D provided by Noranda Inc. (Quebec), (2) AXJ530 alloy developed and provided by General Motors (USA) which is a modified commercial AM50 alloy with addition of 3% Ca and a small amount of Sr; (3) MRI 153 alloy developed by Dead Sea Magnesium Ltd (Israel), which is a modified commercial AZ91 with addition of Ca and Sr, and (4) ZAEX10430 alloy developed at Université Laval (Quebec City, Canada) based on the Mg–Zn–Al system with addition of Ce and Ca.

Our main subject of investigation was the first hydrogenation (activation) of these alloys. It is well known that activation of magnesium is a very slow process and has to be carried out at high temperature and pressure. For commercial product, such expenditure in terms of time and energy translates to higher production cost. Therefore, to reduce cost of magnesium hydride the problem of activation has to be solved. Our hypothesis is that, by inducing important strain and increasing the number of defects, severe plastic deformation techniques could be a way to improve activation in magnesium-based alloys. Even if the magnesium alloys are more expensive than pure magnesium, the alloying elements are expected to hinder the movement of dislocations. Thus, severe plastic deformation (SPD) may lead to greater induced strain and higher number of defects, which makes these alloys easier to activate than pure magnesium. Among the numerous SPD techniques, we choose cold rolling for our investigation because

* Corresponding author. Tel.: +1 819 376 5011x3576; fax: +1 819 376 5164.
E-mail address: jacques.huot@uqtr.ca (J. Huot).

0925-8388/$ – see front matter © 2012 Elsevier B.V. All rights reserved.
doi:10.1016/j.jallcom.2012.01.049

Table 1
Chemical composition of magnesium alloys.

Alloy	Composition (wt.%)						
	Al	Zn	Mn	Ca	Sr	RE	Mg
AZ91D	9.0	0.7	0.25	–	–	–	bal.
AXJ530	4.9	–	0.30	3.0	0.16	–	bal.
MRI 153	8.3	1.0	0.16	0.84	0.1	0.11	bal.
ZAEX10430	3.9	10.4	0.17	0.19	–	2.6	bal.

this is a technique that could be easily scaled up to industrial level.

For purpose of comparison, hydrogen storage properties of as-cast pure magnesium (cut from ingot) were measured and considered as a reference for evaluation with the alloys under consideration.

2. Experimental

The chemical compositions of the cast magnesium alloys used in this study are given in Table 1. Specimens of as-cast magnesium alloys were cut out from ingots. Specimens of die-cast alloys were cut from plates produced by a Bühler high pressure die-cast (HPDC) machine. ZAEX10430 alloy was studied only in the die-cast state since ingots from this alloy were unavailable. As already stated, as-cast pure magnesium (cut from ingot) was considered as a reference alloy in this study. All the as-cast and die-cast specimens (including the as-cast pure magnesium) were cold rolled between two Stainless Steel (316) plates using a Durston DRM 100 rolling mill with rolls of 65 mm diameter and 130 mm length. For each alloy, rolling was performed on a small plate cut from the original ingot. The plates were rolled 50 times in air. After each roll, the plates were fold in two and rolled again thus obtaining a 50% thickness reduction at each rolling pass. Final thickness was about 0.3 mm. After the final roll, the material was mixed with 5 wt.% of MgH_2 and ball milled for 30 min. This ball milling step is essential for activation purpose because it adds nucleation points for the hydride phase. More details about this procedure will be given in a forthcoming paper.

The hydrogen activation and kinetics measurements (absorption and desorption) were carried out in a Sieverts' type apparatus. Specimens were first heated under vacuum at 623 K to insure that the magnesium hydride introduce at the ball milling step was dehydrogenated. Thereafter, the samples underwent an activation treatment at 623 K under hydrogen pressure of 2 MPa for the hydrogenation and 0.01 MPA for the dehydrogenation. A second cycle of hydrogenation/dehydrogenation was then carried out at the same conditions of temperature and hydrogen pressure.

The microstructures of the specimens before rolling were studied by scanning electron microscope (JEOL 840-A). The composition of phases was determined by CAMECA SX-100 electron probe microanalyser (EPMA). The microstructures of the cold rolled specimens before and after the hydrogenation/dehydrogenation cycles were analyzed by X-rays diffraction on a Bruker D8 Focus apparatus with Cu-Kα radiation.

3. Results

3.1. Microstructural characterization

Typical microstructures of as-cast (ingot) magnesium alloys are shown in Fig. 1. The microstructure of as-cast AZ91D which is composed of primary α-Mg grains and discontinuous and divorced $Mg_{17}Al_{12}$ eutectic is shown in Fig. 1A. The white particles are Al_8Mn_5 compound (γ-brass phase). The microstructure of as-cast MRI530 as shown in Fig. 1B is composed of large primary α-Mg grains surrounded by lamellar and divorced eutectic constituents.

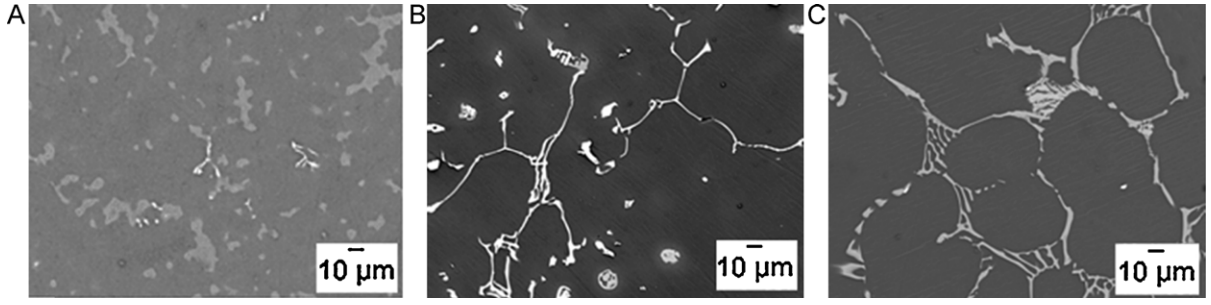

Fig. 1. Microstructures of as-cast (A) AZ91D, (B) MRI153, and (C) AXJ530.

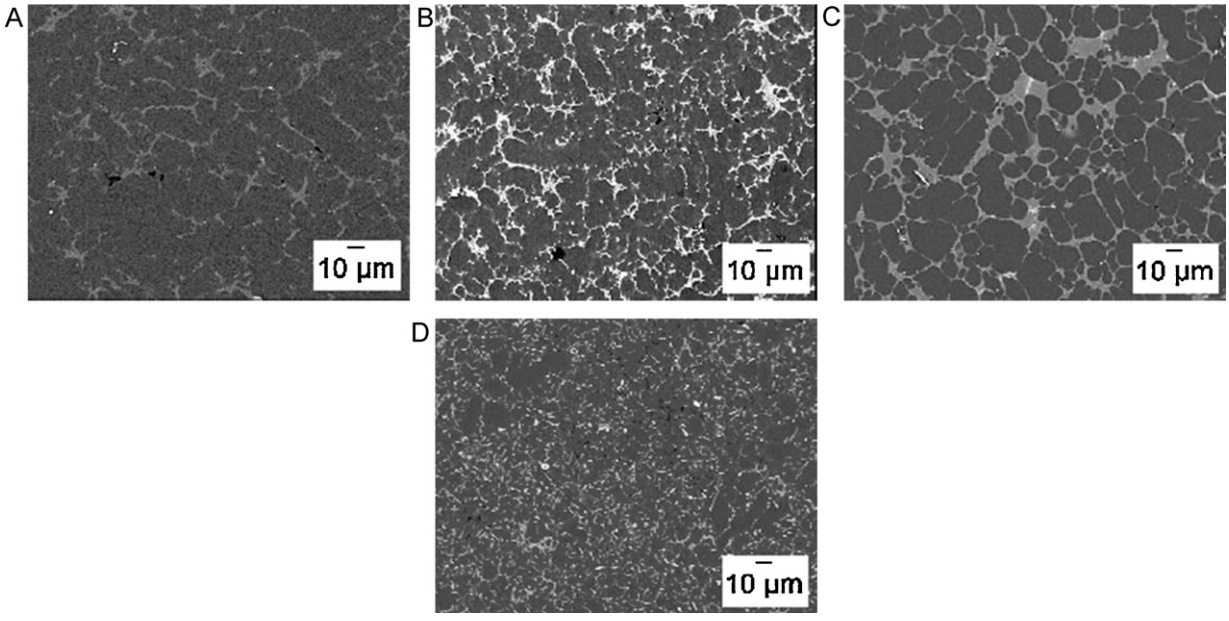

Fig. 2. Microstructures of die-cast (A) AZ91D, (B) MRI153, (C) AXJ530, and (D) ZAEX10430.

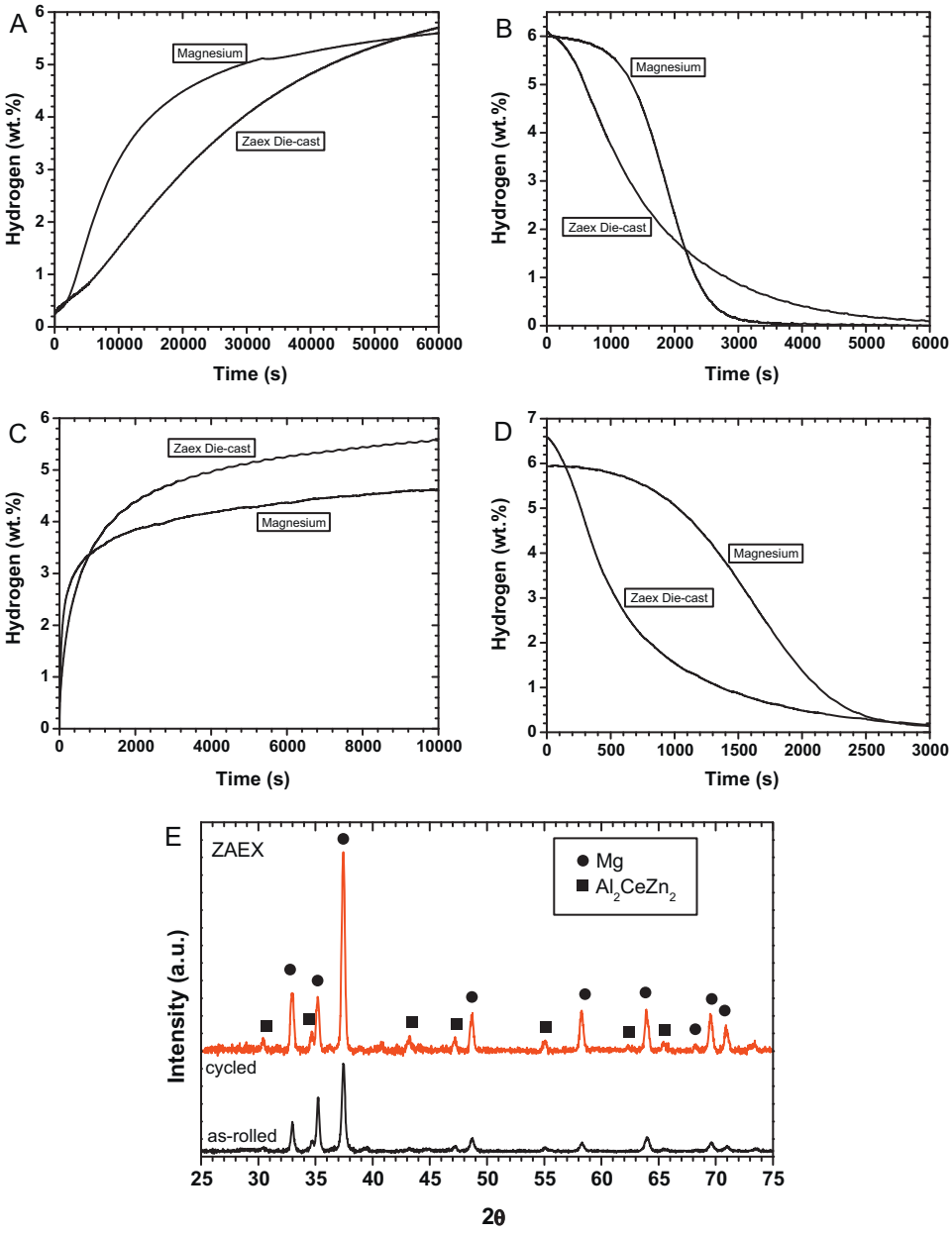

Fig. 3. ZAEX10430 die-cast alloy compared to pure magnesium. First hydrogenation (A); first dehydrogenation (B); second hydrogenation (C); second dehydrogenation (D); and X-ray diffraction patterns after cold rolling and after hydrogenation/dehydrogenation cycle (E).

Eutectics consists in a mixture of $(Mg,Al)_2Ca$ and $(Mg,Al)_2(Sr,Ca)$ phases. The microstructure of as-cast AXJ530 (ingot) is composed of large primary α-Mg grains surrounded by eutectic constituents (Fig. 1C). Two kinds of eutectic structures were observed: coarse lamellae which form the majority of the eutectic structure, and a divorced eutectic. Both lamellar and divorced eutectic consist of Mg–Al–Ca-rich phase, which was identified as $(Mg,Al)_2Ca$ based on XRD and TEM determinations [13–15]. Coarse precipitates containing aluminum and calcium was found within the primary grains. Sr-rich particles were also observed between the α-Mg grains.

Microstructures of die-cast specimens are shown in Fig. 2. Fig. 2A displays the microstructures of die-cast (DC) AZ91D. Die-cast specimens show fine α-Mg grains and α + β ($Mg_{17}Al_{12}$) eutectic at grain boundaries. The microstructures of die-cast MRI 153 specimens as shown in Fig. 2B is composed mostly of α-Mg phase. The eutectic consists of supersaturated α-Mg phase and a $(Mg,Al)_2Ca$ compound. The presence of $(Mg,Al)_2(Sr,Ca)$, described by Sato et al. [16] as having an hexagonal structure, was also found. The microstructure of die-cast AXJ530-DC specimens (Fig. 2C) consists of primary α-Mg dendrites surrounded by eutectic constituent. The eutectic constituent in AXJ530 die-cast is composed by fine α-Mg grains and a $(Mg,Al)_2Ca$ compound having a structure similar to Mg_2Ca [13,14]. Strontium-rich phases (white areas) have been also observed. Typical microstructure of die-cast ZAEX10430 is shown in Fig. 2D. The primary phase consists of a solid solution of Zn and Al in Mg. The interdendritic phases were analyzed by TEM and were found to correspond to the τ phase ($Mg_{32}(Al,Zn)_{49}$) and Al_2CeZn_2 [17]. Very fine particles are presence in the matrix in die-cast specimens. Finally, the presence of fine distribution of Al–Mn particles was noted in all studied alloys.

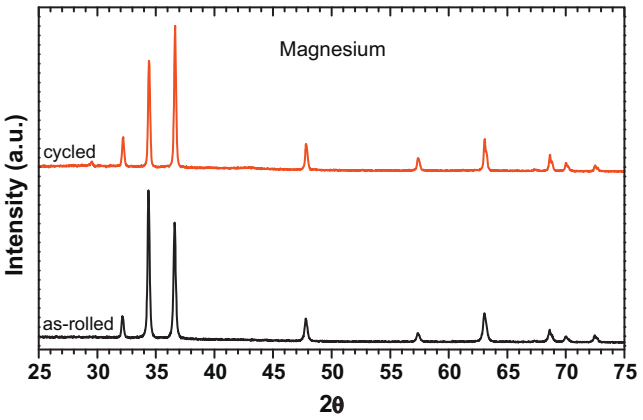

Fig. 4. X-ray diffraction patterns after cold rolling and after hydrogenation/dehydrogenation cycle of as-rolled and after hydrogen cycling of cold rolled pure magnesium.

3.2. ZAEX10430

Fig. 3 shows the hydrogen sorption properties and crystal structure of die-cast ZAEX10430 along with as-cast pure magnesium. Fig. 3A is the activation (first hydrogenation) kinetic and it is obvious that activation kinetic of die-cast ZAEX10430 is slower than that of as-cast pure magnesium. However, the activation step is as complete and the same hydrogen capacity was ultimately obtained. In the first dehydrogenation (Fig. 3B) the kinetic is slower in the case of the ZAEX10430 alloy but it should be noted that it did not present the incubation period observed for pure magnesium. The second hydrogenation and dehydrogenation curves of the two materials are presented in Fig. 3C and D. We see that the hydrogenation kinetics are essentially the same, the only difference being the total capacities. For dehydrogenation, contrary to the first dehydrogenation here the ZAEX10430 alloy is faster than pure magnesium mainly because of the absence of incubation time. But the kinetic is also intrinsically faster for the alloy compared to pure magnesium. The reason for this discrepancy could be found in the crystal structure shown in Fig. 3E. In this figure, the diffraction pattern of ZAEX10430 after cold rolling and after hydrogen cycling is shown. The as-rolled pattern shows that after rolling the (0 0 2) Bragg peak at around 34 degrees is slightly more intense than expected. This is due to preferred orientation induced by rolling. After hydrogen cycling this texture is almost completely lost. In both patterns, the minor phase Al_2CeZn_2 was clearly identified by a series of small peaks. This phase was also seen in TEM investigation. However, no evidence of $Mg_{32}(Al, Zn)_{49}$ phase could be found in the X-ray patterns. The presence of the secondary phase Al_2CeZn_2 may means that this phase is acting as a catalyst for hydrogen sorption.

Here, it should be pointed out that, after cold rolling, pure magnesium plates were also highly textured along (0 0 2) as shown in Fig. 4.

3.3. AXJ530

The hydrogen sorption properties of AXJ530 alloy (as-cast and die-cast) compared to pure magnesium are shown in Fig. 5. On the whole, Fig. 5A and B show that both the first hydrogenation and dehydrogenation kinetic are slower for the two AXJ530 materials as compared to pure magnesium. Especially for desorption, we see that although the incubation time is shorter for the AXJ530 alloys, the intrinsic kinetic is much slower than pure magnesium. This is also seen in the second cycle of absorption desorption sown respectively in Fig. 5C and 5D. The hydrogen capacity of AXJ530 alloy is lower than pure magnesium. However, the hydrogenation kinetics

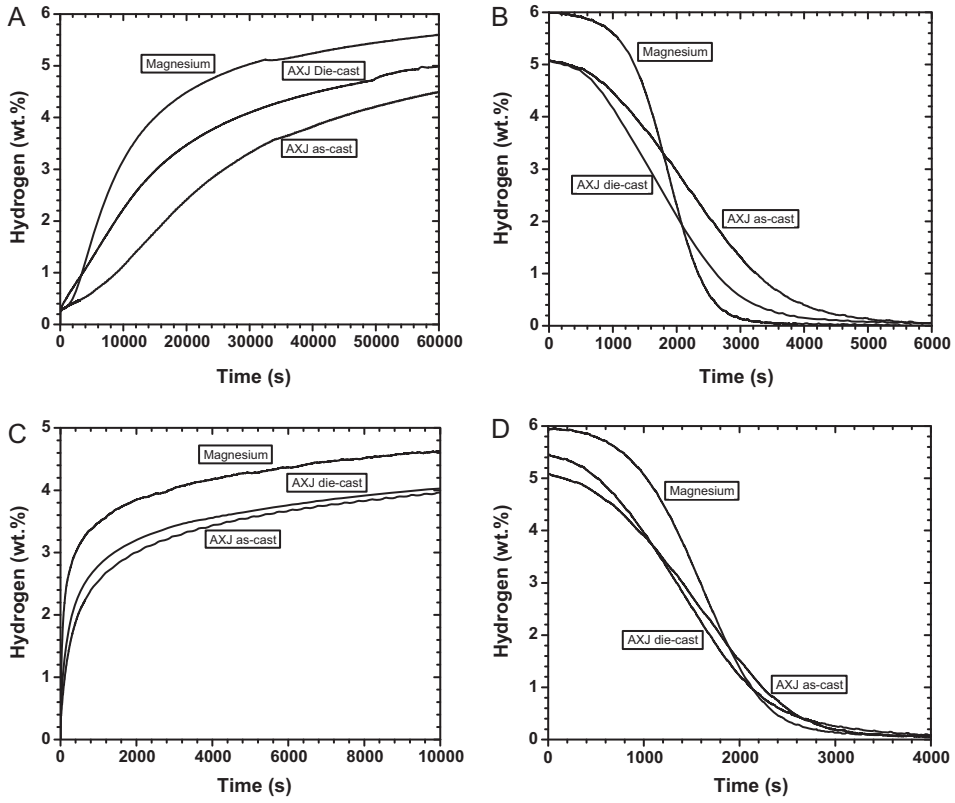

Fig. 5. AXJ530 cast and die-cast alloys compared to pure magnesium. First hydrogenation (A); first dehydrogenation (B); second hydrogenation (C); and second dehydrogenation (D).

are very similar while the dehydrogenation kinetics are still slower than pure magnesium. Still, it is interesting to note that the hydrogenation and dehydrogenation kinetic of die-cast AXJ530 and as-cast (ingot) AXJ530 become roughly similar during this second cycle.

X-ray diffraction patterns of as-cast and die-cast AXJ530 after rolling and after hydrogen cycling are shown in Fig. 6. For both as-cast and die-cast alloys, the as-rolled pattern shows preferred orientation from the (0 0 2) Bragg peak at around 34°. This preferred orientation is almost the same for both alloys. Moreover, one hydrogenation/dehydrogenation cycle did not significantly changed the preferred orientation, contrary to the case of ZAEX10430 where the preferred orientation was totally lost after hydrogen cycling.

3.4. MRI153

Fig. 7A shows the activation of as-cast and die-cast MRI153 alloy, as compared to that of pure (as-cast) magnesium. It is obvious that as-cast MRI153 activate faster than pure magnesium and die-cast MRI153. Thorough inspection of the curves show that, up to a capacity of about 4.5 wt.%, the intrinsic kinetic of the as-cast MRI153 and magnesium is the same, the only difference being the incubation time which is absent in the case of as-cast alloy. For higher capacity, the activation kinetic of as-cast alloy is faster than for pure magnesium. In the case of die-cast alloy, we see a long incubation time up to about 1400 s. Afterward, the kinetic is getting gradually faster and after about 3000 s the as-cast and die-cast kinetics are the same.

The first dehydrogenation of is presented in Fig. 7B. It can be seen that as-cast and die-cast MRI153 have quite similar desorption kinetic the only difference is that the as-cast alloy has a higher hydrogen capacity because it has been more completely activated. Pure magnesium has a long incubation time (about 1000 s) while the two MRI alloys immediately started to desorb hydrogen.

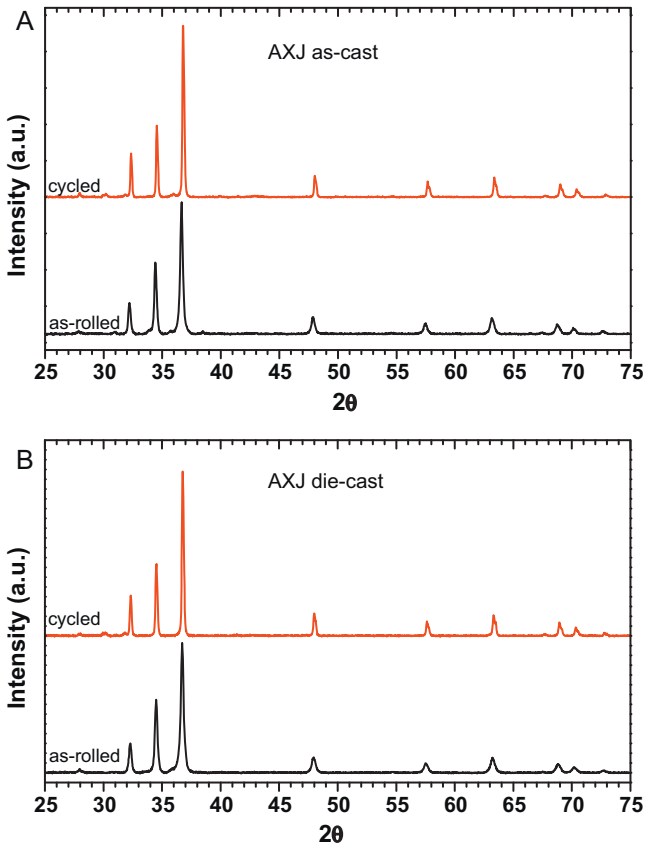

Fig. 6. X-ray diffraction patterns after cold rolling and after hydrogenation/dehydrogenation cycle of cast (A) and die-cast (B) AXJ530 alloy. All Bragg peaks belong to Mg phase.

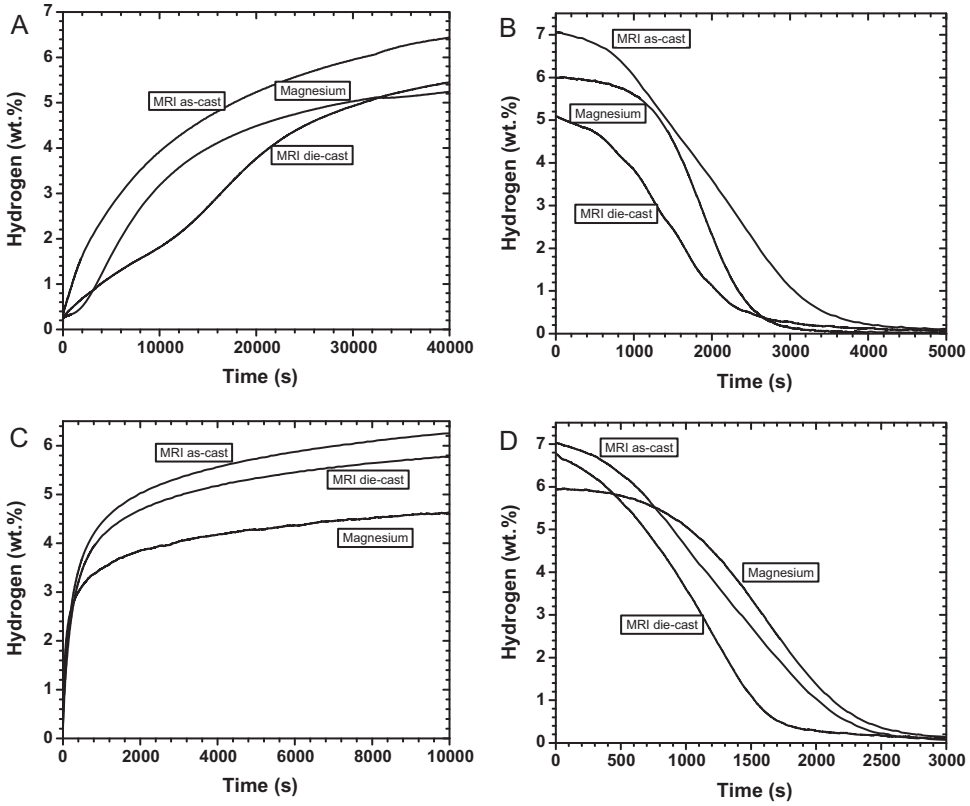

Fig. 7. MRI153 cast and die-cast alloys compared to pure magnesium. First hydrogenation (A); first dehydrogenation (B); second hydrogenation (C); and second dehydrogenation (D).

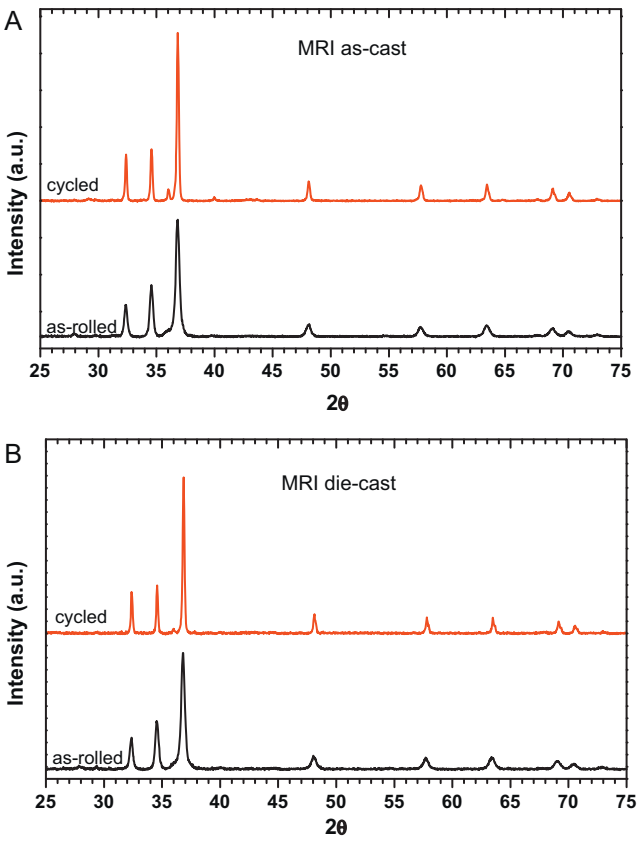

Fig. 8. X-ray diffraction patterns after cold rolling and after hydrogenation/dehydrogenation cycle of cast (A) and die-cast (B) MRI153 alloy. All Bragg peaks belong to Mg phase.

However, after the incubation period the pure magnesium kinetic is faster.

Second hydrogenation and dehydrogenation curves of the two MRI153 materials and the pure magnesium are presented in Fig. 7C and D, respectively. We see that the initial absorption kinetic (Fig. 7C) is the same for the three compounds. The difference is that this initial kinetics goes up to higher hydrogen capacity for the two MRI alloys than for pure magnesium. All compounds then go into a second kinetic regime which is much slower than the first one but again the second regime kinetic is essentially the same for the three compounds. In the case of desorption (Fig. 7D), pure magnesium curve is almost identical to the one of the first cycle (Fig. 7B). The two MRI samples do not show incubation period, as in Fig. 7B, but here their intrinsic kinetic is almost the same as pure magnesium, contrary to the first cycle. Thus, the end result is that both samples fully desorbs faster than pure magnesium even if their total capacity is higher.

X-ray diffraction patterns of MRI153 alloys are shown in Fig. 8. Here, there is almost no preferred orientation in the as-rolled samples. There is also a minimal difference in the as-rolled and after cycling patterns for both as-cast and die-cast alloys.

3.5. AZ91D

Activation (first hydrogenation) of AZ91D as-cast (ingot) and die-cast specimens compared to pure magnesium is shown in Fig. 9A. It is clear that the activation of as-cast AZ91D is faster than that of the pure magnesium, while the die-cast AZ91D showed the slowest activation rate mainly because of an incubation time of about 6000 s.

The dehydrogenation performed after the activation step is presented in Fig. 9B. It could be seen that the first dehydrogenation of the AZ91D as-cast is faster than that of pure magnesium, while the die-cast AZ91D showed once again the slowest desorption rate.

Fig. 9C shows the second hydrogenation of the AZ91D as-cast and die-cast specimens, as well as for the pure magnesium. On the whole, the three materials exhibited a faster kinetic than that showed during activation and seems to have the same intrinsic kinetics. The main difference is the total capacity achieved. This is due to the degree of activation achieved by each alloy in the activation step shown in Fig. 9A. The fact that all absorption kinetics are quite similar is understandable as all samples are basically magnesium. Thus, the beneficial effect of using AZ91D is mainly seen for the activation step which is faster and gives a higher capacity than pure magnesium.

Fig. 9D displays the second dehydrogenation of the two AZ91D specimens and of the pure magnesium. Here again, the intrinsic kinetic of pure magnesium and AZ91D die-cast are almost identical. However, the as-cast AZ91D showed faster kinetic than the other two materials. Therefore, it seems that some catalytic activities are present in the alloy (Fig. 10).

4. Discussion

Among the alloys investigated, the as-cast forms of AZ91D and MRI153 presented faster activation kinetics than pure magnesium. However, the die-cast form of these two alloys was actually slower to activate than pure magnesium. Second hydrogenation leads to a significant improvement of the absorption kinetic of both as-cast and die-cast AZ91D and MRI153, as compared to as-cast pure magnesium. It is worthwhile to notice that once again, the as-cast AZ91D and MRI153 showed faster absorption kinetic that the die-cast materials.

Since both AZ91D and MRI153 alloys contain about 9 wt.% of aluminum, the improvement of hydrogen storage properties of both materials as compared to that of pure magnesium may be attributed to the addition of this alloying element to magnesium. However, the effect of aluminum addition on the (quite similar) hydrogen storage properties of AZ91D and MRI153 must be analyzed thoroughly, due to some microstructural differences between the two alloys. While the matrix for both alloys consists of primary α-Mg phase, the composition and microstructure of secondary phases are different. In fact, in AZ91D alloy a compound of α-Mg + β ($Mg_{17}Al_{12}$) eutectic is formed at grain boundaries, while in MRI153, the eutectic consists of supersaturated α-Mg phase and a $(Mg,Al)_2Ca$ compound, with the presence of $(Mg,Al)_2(Sr,Ca)$ and small amount of $Mg_{17}Al_{12}$. On the other hand, as-cast alloys are characterized by a ratio of primary α-Mg phase to secondary phases which is higher than that of die-cast alloys. Finally, due to the higher solidification rate experienced by die-cast alloys, the primary α-Mg phase present in die-cast AZ91D and MRI153 contains less segregation than their as-cast form.

Thus, given that AZ91D and MRI153 alloys have similar matrix (primary α-Mg phase) whatever the casting process (ingot or die casting), their similar hydrogen storage properties can be attributed mainly to the hydrogenation/dehydrogenation kinetic of the primary α-Mg phase. This hypothesis can explain the better hydrogen storage properties of as-cast specimens as compared to die-cast ones, since the fraction of primary α-Mg phase is higher in as-cast than in die-cast specimens. We can then argue that hydrogen storage occurs mainly in primary α-Mg phase. However, the role played by secondary phases in both alloys on their hydrogen storage properties need to be studied further.

The difference of hydrogen storage properties of as-cast and die-cast specimens during the first cycle might be attributed to the

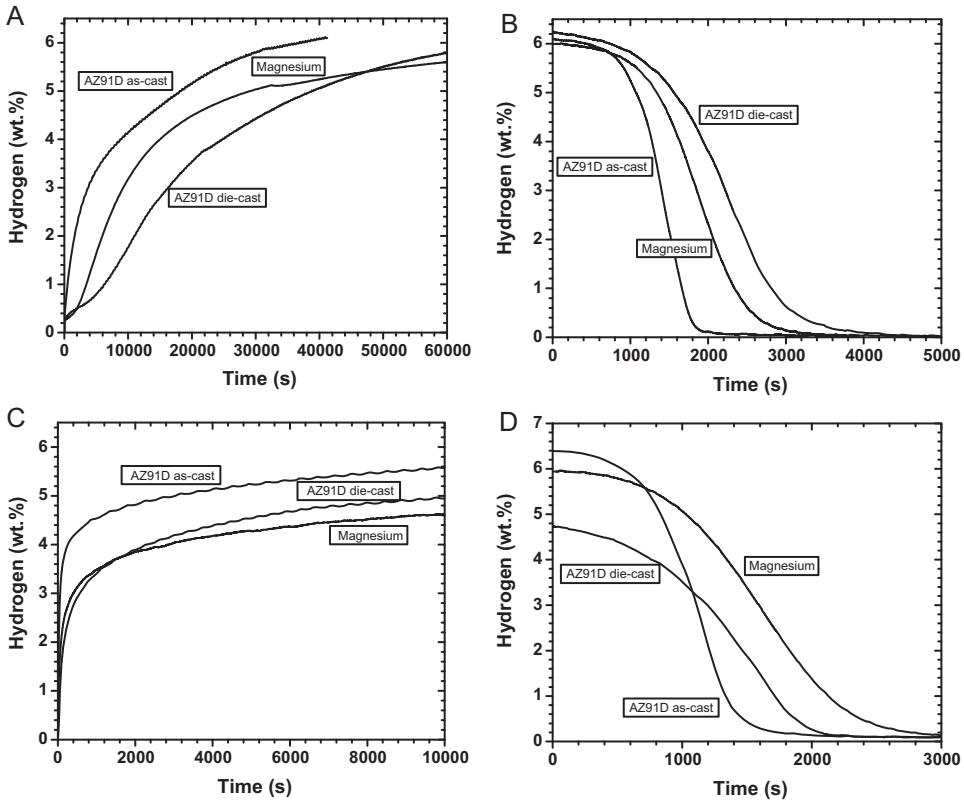

Fig. 9. AZ91D cast and die-cast alloys compared to pure magnesium. First hydrogenation (A); first dehydrogenation (B); second hydrogenation (C); and second dehydrogenation (D).

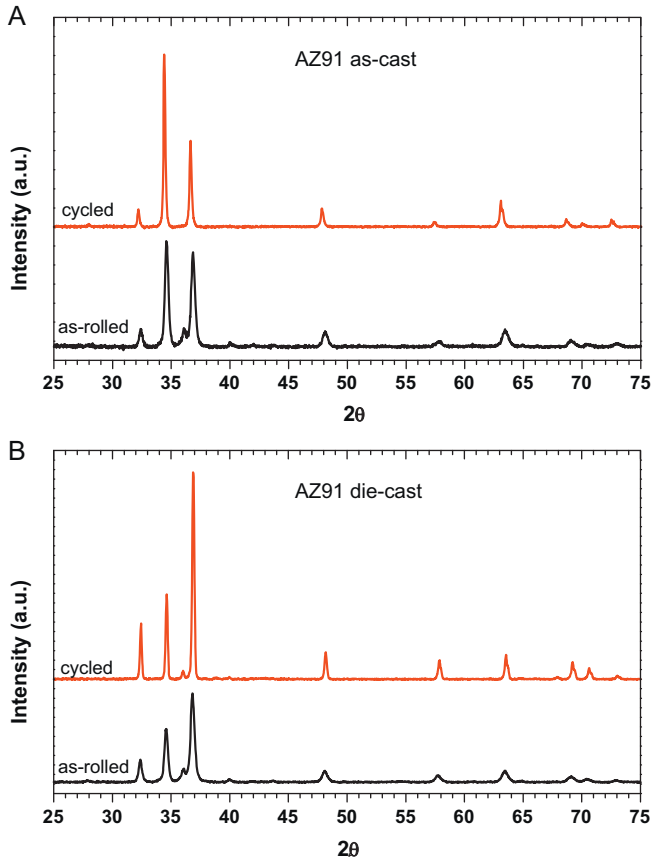

Fig. 10. X-ray diffraction patterns after cold rolling and after hydrogenation/dehydrogenation cycle of cast (A) and die-cast (B) AZ91D alloy. All Bragg peaks belong to Mg phase.

level of segregation inside the primary α-Mg phase. This difference is lower during the second cycle because the distribution of aluminum inside the primary α-Mg phase become homogenous and probably similar in both as-cast and die-cast specimens caused by the diffusion of aluminum atoms which is promoted by heating at high temperatures.

The other cold rolled magnesium alloy which showed interesting hydrogen storage properties in this study is the die-cast ZAEX10430. Although the first hydrogenation/dehydrogenation kinetic of die-cast ZAEX10430 was slower compared to as-cast pure magnesium, the second hydrogenation/dehydrogenation kinetic was faster and roughly equivalent to those of die-cast AZ91D and MRI153. The presence of Zn and Al in the matrix of the die-cast ZAEX10430 might explain these interesting hydrogen storage properties, but this effect has to be further studied. It is possible also that the finely dispersed secondary phases as shown in Fig. 2d promote the nucleation of the hydride phase.

The AXJ530 magnesium alloys showed the worst hydrogen storage properties among all the studied alloys during both the first and second hydrogenation/dehydrogenation cycles. During the first hydrogenation/dehydrogenation, die-cast AXJ530 showed better kinetic than as-cast AXJ530. This behavior is quite the opposite of that showed by AZ91D, MRI153 and ZAEX1043 where the as-cast material displays better absorption/desorption kinetic than the die-cast one, especially during the first cycle. We suspect the effect of the coarse precipitates formed in as-cast AXJ530 (see Fig. 1b) on its poor hydrogenation/dehydrogenation kinetic especially during the first cycle.

5. Conclusion

In this work, we have shown that all the studied magnesium alloys, except AXJ530, showed on the whole better hydrogen

storage properties than as-cast pure magnesium, especially during the second dehydrogenation.

Both AZ91D and MRI153 materials show quite similar absorption/desorption properties. As-cast (ingot) AZ91D and MRI153 showed faster hydrogenation/dehydrogenation kinetic that the die-cast materials, mainly during the second cycle. For MRI the improvement could not be related to structural changes because they are minimal. For AZ91 there is the biggest change in structure (preferred orientation) and this could play a role in enhancement of hydrogen storage. A major role is probably played by the secondary phases at the grain boundaries. This should be investigated more deeply.

Die-cast ZAEX10430 showed slow first hydrogenation/dehydrogenation kinetic. During the second cycle, the hydrogen storage properties of die-cast ZAEX10430 improved markedly and became similar to those of AZ91D and MRI153 alloys.

The AXJ530 magnesium alloys showed the worst hydrogen storage properties among all the studied alloys during both the first and second hydrogenation/dehydrogenation cycles.

The discrepancies between as-cast and die-cast alloys point means that phase segregation plays an important role in the hydrogen storage properties of magnesium-based alloys. This phenomenon should be studied further.

Our results have shown that for some magnesium alloys the first hydrogenation (activation) is faster than pure magnesium. As activation is a major problem for industrial synthesis of magnesium hydride we think that using magnesium alloys instead of pure magnesium may decrease the production cost of magnesium hydride and open new markets for the use of this hydride.

Acknowledgments

This work was supported by fundings from Natural Science and Engineering Council of Canada. S. Amira gratefully thanks Hydro-Quebec for a post-doctoral fellowship. The authors would like to thanks Prof. E. Ghali of the *Département de génie des mines, de la métallurgie et des matériaux* of Université Laval for kindly providing us with the magnesium alloys used for this study.

References

[1] DOE/FCT, DOE Targets for On-Board Hydrogen Storage Systems for Light-Duty Vehicles, 2009, http://www1.eere.energy.gov/hydrogenandfuelcells/storage/pdfs/targets_onboard_hydro_storage.pdf.
[2] T. Vegge, L.S. Hedegaard-Jensen, J. Bonde, T.R. Munter, J.K. Norskov, Trends in hydride formation energies for magnesium-3d transition for metal alloys, Journal of Alloys and Compounds 386 (2005) 1.
[3] T. Sato, H. Blomqvist, D. Noréus, Attempts to improve Mg_2Ni hydrogen storage by aluminium addition, Journal of Alloys and Compounds 356/357 (2003) 494.
[4] M.Y. Song, Effects of mechanical alloying on the hydrogen storage characteristics of Mg–*x*wt% Ni (*x* = 0, 5, 10, 25 and 55) mixtures, International Journal of Hydrogen Energy 20 (1995) 221.
[5] M.-Y. Song, S.-H. Hong, I.-H. Kwon, S.-N. Kwon, C.-G. Park, J.-S. Bae, Improvement of hydrogen-storage properties of Mg by reactive mechanical grinding with Fe_2O_3 prepared by spray conversion, Journal of Alloys and Compounds 398 (2005) 283.
[6] M. Au, Hydrogen storage properties of magnesium based nanostructured composite materials, Materials Science and Engineering B 117 (2005) 37.
[7] L.T. Zhang, K. Ito, V.K. Vasudevan, M. Yamaguchi, Hydrogen absorption and desorption in a B2 single-phase Ti–22Al–27Nb alloy before and after deformation, Acta Materialia 49 (2001) 751.
[8] L.T. Zhang, K. Ito, V.K. Vasudevan, M. Yamaguchi, Effects of cold-rolling on the hydrogen absorption/desorption behavior of Ti–22Al–27Nb alloys, Materials Science and Engineering A 329/331 (2002) 362.
[9] T.T. Ueda, M. Tsukahara, Y. Kamiya, S. Kikuchi, Preparation and hydrogen storage properties of Mg–Ni–Mg_2Ni laminate composites, Journal of Alloys and Compounds 386 (2004) 253.
[10] J. Dufour, J. Huot, Rapid activation, enhanced hydrogen sorption kinetics and air resistance in laminated Mg–Pd2.5at.%, Journal of Alloys and Compounds 439 (2007) L5.
[11] J. Dufour, J. Huot, Study of Mg_6Pd alloy synthesized by cold rolling, Journal of Alloys and Compounds 446/447 (2007) 147.
[12] L. Guoxian, W. Erde, F. Shoushi, Hydrogen absorption and desorption characteristics of mechanically milled Mg–35wt.%FeTi1.2 powders, Journal of Alloys and Compounds 223 (1995) 111.
[13] A.A. Luo, M.P. Balogh, B.R. Powell, Tensile Creep and Microstructure of Magnesium-Aluminum-Calcium Based Alloys for Powertrain Applications—Part 2 of 2. SAE 2001 World Congress, SAE, Detroit, MI, USA, 2001.
[14] B.R. Powell, A.A. Luo, V. Rezhets, J.J. Bommarito, B.L. Tiwari, Development of Creep-resistant Magnesium Alloys for Powertrain Applications: Part 1 of 2. SAE 2001 World Congress, SAE, Detroit, MI, USA, 2001.
[15] A. Suzuki, N.D. Saddock, J.W. Jones, T.M. Pollock, Structure and transition of eutectic (Mg,Al)2Ca Laves phase in a die-cast Mg–Al–Ca base alloy, Scripta Materialia 51 (2004) 1005.
[16] T. Sato, B.L. Mordike, J.F. Nie, M.V. Kral, An electron microscope study of intermetallic phases in AZ91 alloy variants, 2005, p. 435.
[17] S. Amira, Influence of microstructure on corrosion behavior and mechanical properties of some creep resistant magnesium alloys, Ph.D. thesis, Université Laval, Quebec city, Canada, 2008, p. 320.